ASM Sc. J., 20(1), 2025
https://doi.org/10.32802/asmscj.2025.1933

Point Spread Function Profile in Human Myopic Model Eye

S.F. Othman[1,2,3*], N. Tamchek[1], F.D. Muhammad[1], A. Abdul Latif[1] and M.H. Ithnin[2]

[1]*Department of Physics, Faculty of Science, Universiti Putra Malaysia, 43400 UPM Serdang, Selangor, Malaysia*

[2]*Ophthalmic Sciences Research Group (OSReG), Department of Optometry & Visual Science, Kulliyyah of Allied Health Sciences, International Islamic University Malaysia, Jalan Sultan Ahmad Shah, Bandar Indera Mahkota, 25200 Kuantan, Pahang, Malaysia*

[3]*SEGi EyeCare, SEGi University, No. 9, Jalan Teknologi, Taman Sains Selangor, Kota Damansara, PJU 5 , 47810 Petaling Jaya, Selangor, Malaysia*

Heretofore, eye modelling is based on the emmetropic eye taking its ocular optical components value from the population-based studies. Howbeit, the effect of aberration of myopic refractive error by modelling the eye using the parameters from ocular biometrics and ray tracing method has not been systematically studied. An objective of this study was to determine the point spread function (PSF) of myopic refractive error using eye modelling and ray tracing technique. Three eye models had been successfully modelled in Zemax software, scilicet, emmetropic Liou and Brennan, myopic Liou and Brennan, and corrected myopic Liou and Brennan. The optical performance of the eye models was analysed using PSF, whereby the PSF is presented in the form of Strehl ratio. A comparison of the two results reveals the Strehl ratio value for myopic Liou and Brennan eye was the lowest compared to its emmetropic model. Further analysis shows that the Strehl ratio of the corrected myopic Liou and Brennan model was higher compared to the uncorrected myopic model. Natheless, the corrected myopic model produced lower Strehl ratio value compared with the emmetropic model of Liou and Brennan. From this research, the accuracy of the Strehl ratios for myopia correction and emmetropia were calculated. It has shown that the accuracy of the Strehl ratio value for corrected myopia was lower.

Keywords: model eye; myopia; optical performance; point spread function; Strehl ratio

I. INTRODUCTION

The vision that's created by the human eye is a result from light encroaches through the complex built in of visual optical components. Hence, the eye model (schematic) that is simpler than the real eye has been designed due to the complexity of the optics of a real eye (Thibos & Bradley, 1999; Zapata-Diaz *et al.,* 2019). Eye models are available with a range of complexity, but at minimum, they include numerical values for radii of curvature, distance between refracting surfaces, and indices of refraction.

Previous myopia studies have proven that myopic refractive error is associated with eyeball elongation, in particular, the vitreous chamber depth increment (Gwiazda *et al.*, 2002; Jiang & Woessner, 1996; Sun *et al.*, 2015). In a routine optometric examination, clinical refraction has been regarded as the conventional way of obtaining myopic refractive error. These clinical refraction techniques, namely, autorefraction, retinoscopy and subjective refraction have been regarded as the standard procedures (Carlson & Kurtz, 2016; Elliot, 2020). Nevertheless, only few studies have been conducted to study the effect of aberration of myopic refractive error by modelling the eye using the parameters obtained from the ocular biometrics and ray tracing method (Hiraoka *et al.,* 2017; Liu & Wang, 2019). Almost all the eye

*Corresponding author's e-mail: shahfarez@iium.edu.my

modelling is based on emmetropic eye. However, no studies have been done to study the effect of aberration of myopia by modelling the eye using the parameters from ocular biometrics and ray tracing method. At present, the eye modelling is based on emmetropic eye. Hence, a question arises whether a computer modelling of eye could be developed to verify the axial type of myopia from the clinical refraction findings, using the numerical values of the parameters of ocular optical components and the fixed refractive indices of media from the existing chosen eye model. In addition, the value of spectacle refractive error is used to correct the myopic eye model and analyse its optical performance using the merit function in Zemax, i.e., the point spread function (PSF) analysis.

This study aimed to assess the aberrations of the image quality of myopia, i.e., the PSF using a ray tracing technique of an eye model.

II. MATERIALS AND METHOD

The research followed the tenets of the Declaration of Helsinki, with the research approved by the Ethics Committee for Research Involving Human Subjects of Universiti Putra Malaysia (UPM) (FS-Jun 13(01) EXP) and with informed consent obtained from all subjects. The study cohort comprised 34 myopic subjects aged 21.80 ± 2 years, ranging from 18 to 36 years. Cycloplegic monocular sphero-cylinder refraction was performed on both eyes using a Jackson crossed-cylinder on a trial frame. Maximum plus and binocular balance to ±0.25 D were administered. The mean spherical equivalent refraction (SER) obtained from the clinical refraction technique was -4.47 ± 1.93 D, ranging from -2.25 D to -9.75 D. The SER covered the degree of myopia from moderate to high which contributes to the elongation of the eyeball, particularly the vitreous chamber depth (Gwiazda *et al.*, 2002). This was measured at 15 mm vertex distance. The onset of myopia must be before the age of 16 years to ensure the myopia was axial in nature, i.e., the so-called juvenile-onset myopia (Bullimore *et al.,* 1992; Chua *et al.,* 2018; Grosvenor & Scott, 1991; McBrien & Millodot, 1987; Zadnik & Mutti, 2019). Subjects with greater than 0.75 D of astigmatism as measured by subjective refraction or with a corrected visual acuity poorer than 6/6 in the test eye were excluded. Subjects were also excluded if they had any ocular disease in either eye, previous ocular surgery, or had intraocular pressure greater than 21 mmHg. Effective pupil diameter (EPD) measurements were taken with undilated pupils. Mean EPD was 2.59 ± 0.43 mm with a range of 2 - 4 mm. The comparison phacometry measurement was conducted to determine the anterior and posterior crystalline lens curvatures. This was followed by keratometry to determine the anterior corneal curvature. Whereas the A-scan ultrasound biometry technique was carried out to determine the parameters of anterior chamber depth, lens thickness and axial length.

The eye modelling was carried out using Zemax software (Zemax, 2012). The modelling is based on previous models of unaccommodated Liou and Brennan emmetropic eyes (Liou & Brennan, 1997). Firstly, the validating of emmetropic eye using computer model utilising clinical ocular parameter from the population-based study was carried out (Liou & Brennan, 1997). Secondly, the optical performance, i.e., the PSF was used in the validation process. Finally, a simple comparison will be proposed to make the validation process would be easy to be utilised in real application of correcting myopic problem.

The PSF is related to the calculation of wavefront aberration using the technique of Fourier transform (Atchison, 2023). The PSF is the results of luminance distribution in the image surface of a light point source. The Strehl intensity ratio, E, is a measure of the effect of aberrations on reducing the maximum or peak value of the PSF. It is defined as follows:

$$E = \frac{Max\ light\ level\ value\ of\ aberrated\ PSF}{Max\ light\ level\ value\ of\ unaberrated\ PSF} \qquad (1)$$

The Strehl intensity ratio has an advantage over the half-width by always being a single number, even if the PSF is not rotationally symmetric. Since the effect of aberrations is to spread out the PSF and decrease the maximum peak height, the Strehl intensity ratio is always less than or equal to one. The greater the aberrations, the lower the value of the Strehl intensity ratio and the poorer the image quality. Even for small aberrations, which do not affect the extension of the PSF, the light intensity in the centre peak can drop significantly (Figure 1). A Strehl ratio $E \geq 0.8$ is generally considered to correspond to diffraction-limited performance (Ottevaere & Thienpont, 2005).

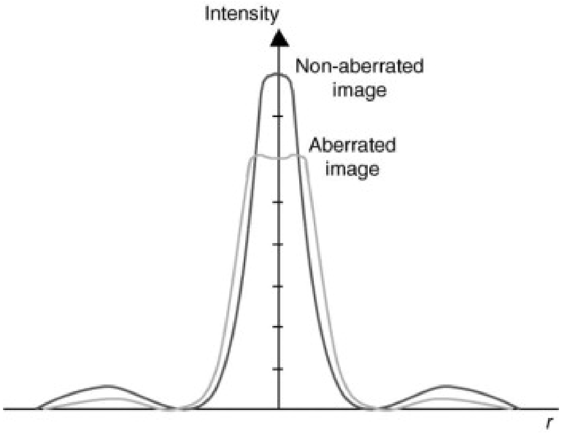

Figure 1. Strehl ratio criterion

The optical parameters of Liou and Brennan emmetropic and myopic eye models were entered in the Zemax's Lens Data Editor in the forms of rows and columns as shown in Table 1 and Table 2 respectively.

Table 1. Ocular parameters input of Liou and Brennan emmetropic eye model in lens editor of Zemax

Surface	Radius (mm)	Thickness (mm)	Refractive Index	Asphericity
1	Infinity	50.00	-	0.00
2	7.77	0.50	1.376	-0.18
3	6.40	3.16	1.336	-0.60
4	Infinity	0.00	1.336	0.00
5	12.40	1.59	Grad A	-0.94
6	Infinity	2.43	Grad P	0.00
7	-8.10	16.27	1.336	0.96
8	-12.00	-	-	0.00

Table 2. Ocular parameters input of Liou and Brennan myopic eye model in lens editor of Zemax

Surface	Radius (mm)	Thickness (mm)	Refractive Index	Asphericity
1	Infinity	50.00	-	0.00
2	7.56	0.50	1.376	-0.18
3	6.40	3.40	1.336	-0.60
4	Infinity	0.00	1.336	0.00
5	11.86	1.79	Grad A	-0.94
6	Infinity	2.00	Grad P	0.00
7	-7.26	16.98	1.336	0.96
8	-12.00	-	-	0.00

An ophthalmic lens was designed by adding an eyeglass lens to the front of the Liou and Brennan myopic eye model. The lens power was taken as -4.47 D using the mean SER results calculated from the clinical refraction technique. This lens power was optimised to provide good imaging quality as the Liou and Brennan emmetropic model eye.

First, two surfaces between the Input Beam (Surface 1) and the Cornea (Surface 2) were inserted. These two surfaces represent the front and back surfaces of the ophthalmic lens. The ophthalmic lens was placed 15 mm from the eye. This 15 mm distance was chosen as a vertex distance from the anterior corneal apex to the back surface of the spectacle plane. The new surfaces, namely, Surfaces 2 and 3 are the front and back surfaces of the ophthalmic lens with a standard surface type. The lens had a thickness of 3 mm with a semi-diameter (radius) of 20 mm. The lens was selected as a polycarbonate material from the Glass Catalogue in Zemax (Zemax, 2012). The refractive index of the material is 1.58547 calculated at 581.1 nm wavelength using Sellmeier Equation as follows, i.e.:

$$n^2 - 1 = \frac{1.4182\lambda^2}{\lambda^2 - 0.021304}, \qquad (2)$$

whereby n is the refractive index of the ophthalmic lens, and λ is the light wavelength.

The equiconcave lens type was chosen for the myopia correction. The radius of curvatures for front and back surfaces were taken as -261.96 mm and +261.96 mm obtained from the following power of Lens Maker's Equation (Tunnacliffe & Hirst, 1996),

$$F = (n_p - 1)\left(\frac{1}{r_1} - \frac{1}{r_2}\right), \qquad (3)$$

where F is the power of the corrective lens used, n_p is the refractive index of the lens, r_1 and r_2 are the radius of curvature of front and back surfaces, respectively. Table 3 summarise the Zemax Lens Data Editor using parameters of Liou and Brennan corrected myopic eye model.

Table 3. Ocular parameters input of Liou and Brennan corrected myopic eye model in lens editor of Zemax

Surface	Radius (mm)	Thick-ness (mm)	Refractive Index	Asphericity
1	Infinity	50.00	-	0.00
2	-261.96	3.00	1.58547	0.00
3	+261.96	28.00	-	0.00
4	7.56	0.50	1.37600	-0.18
5	6.40	3.40	1.33600	-0.60
6	Infinity	0.00	1.33600	0.00
7	11.86	1.79	Grad A	-0.94
8	Infinity	2.00	Grad P	0.00
9	-7.26	16.98	1.33600	0.96
10	-12.00	-	-	0.00

Finally, once the optical performances were achieved, the results were analysed and presented. The result from the modelling was then compared with each eye models. The finding from the comparison study was used to confirm on how optical performance of a myopic eye could be validated when it was in uncorrected and corrected status.

III. RESULT AND DISCUSSION

The 2-D layout of the emmetropic Liou and Brennan eye model from Zemax output is presented in Figure 2. The Liou and Brennan model refracting surfaces are shown accordingly starting from infinity to the anterior cornea, posterior cornea, anterior lens and posterior lens. According to Liou and Brennan model, the retinal curvature was taken into consideration for image formation (Smith *et al.*, 2008).

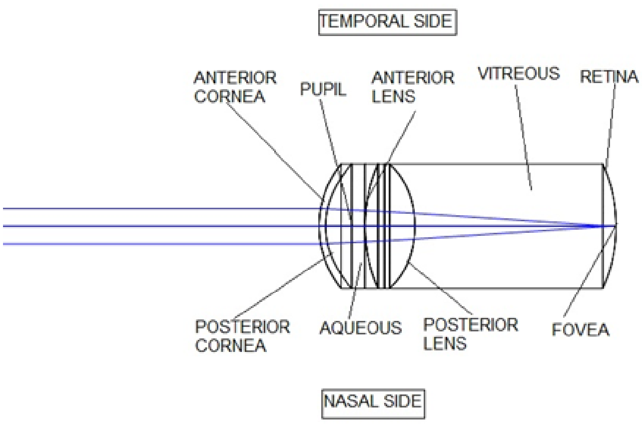

Figure 2. 2-D layout of emmetropic Liou and Brennan eye model

Table 4 shows the Strehl ratio values for emmetropic Liou and Brennan eye model with different wavelengths.

Table 4. The Strehl ratio for emmetropic Liou and Brennan eye model with different wavelengths

Model	**Wavelength (nm)**		
	486.1	**587.6**	**656.3**
Liou & Brennan	0.824	0.931	0.846

An inspection of the data in Table 4 reveals that the Strehl ratio increases along with the increment of the wavelengths. The Strehl ratio for emmetropic Liou and Brennan is greater than 0.8 which indicates this model has a diffraction limited characteristic (Ottevaere & Thienpont, 2005). However, the increasing tendency is slower, and the pattern is not in a linear fashion. The Strehl ratio of the green wavelength is higher than the red. This could be due to the green wavelength, i.e., 587.6 nm being closer to the human peak luminosity at 555 nm (Freeman & Hull, 2003; Chen *et al.*, 2018).

The 2-D layout of the myopic Liou and Brennan eye model from Zemax output is presented in Figure 3. The myopic Liou and Brennan model refracting surfaces are shown accordingly starting from infinity to the anterior cornea, posterior cornea, anterior lens and posterior lens.

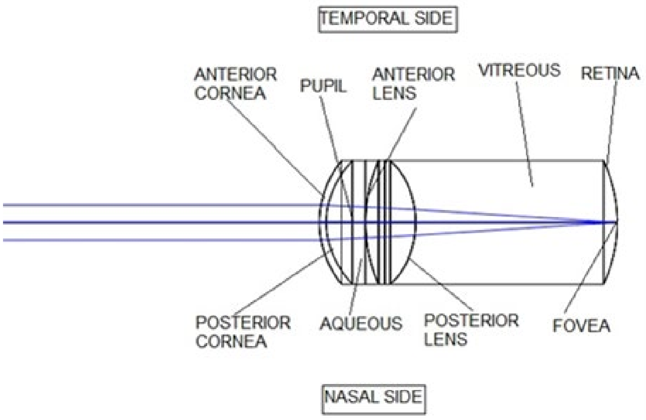

Figure 3. 2-D layout of myopic Liou and Brennan eye model

The Strehl ratio values for blue, green and red wavelength colours of this myopic Liou and Brennan model were 0.003, 0.003 and 0.004 respectively. The Strehl values for the blue and green wavelengths were the same and almost akin to the red. As the Strehl values were very small and similar among the 3 wavelengths, it showed that the PSF for the myopic Liou and Brennan model were significantly aberrated. The Strehl ratio for myopic Liou and Brennan eye models are shown in Table 5.

Table 5. Strehl ratio for myopic Liou and Brennan eye model with different wavelengths

Model	**Wavelength (nm)**		
	486.1	**587.6**	**656.3**
Liou & Brennan	0.003	0.003	0.004

Moving on, in comparison with the Strehl ratio on other emmetropic eye models as shown in Table 4, it was found out that the Strehl ratio value of myopic Liou and Brennan were much lower. Most of the parameters used to model the myopic version of the Liou and Brennan eye were taken from the mean parameters of ocular biometry from the real myopic subjects, which made the model far from a diffraction-limited PSF. Therefore, the Strehl ratio obtained from the myopic Liou and Brennan indicates that the aberrated PSF width was wider, and the crest height is reduced compared to the emmetropic models (Collins, Buehren & Iskander, 2006; He *et al.*, 2005). Moreover, as the ocular dimensions of the myopic eye revealed the status of an uncorrected refractive error, ergo the final image is not formed on the retina. Thus, it showed that the final image was defocused, aberrated and scattered.

The 2-D layout of the corrected myopic Liou and Brennan eye model from Zemax output is presented in Figure 4. The corrected myopic Liou and Brennan model refracting surfaces are shown accordingly starting from infinity to the anterior cornea, posterior cornea, anterior lens and posterior lens. The concave lens used to correct myopic refractive error was positioned in front of the eye at a vertex distance of 15 mm. The vertex distance is a distance from the anterior corneal surface to the back surface of the lens.

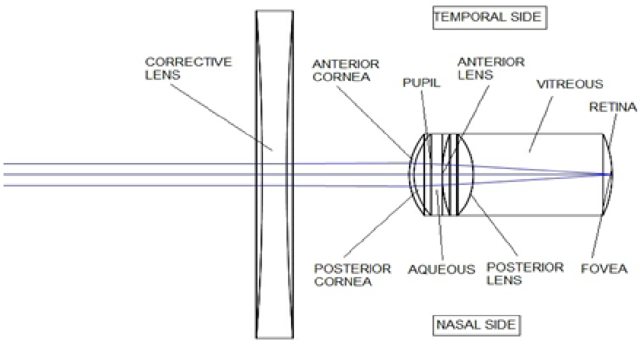

Figure 4. 2-D layout of corrected myopic Liou and Brennan eye model

The Strehl ratio for emmetropic and corrected myopic of Liou and Brennan eye models are shown in Table 6.

Table 6. Strehl ratio for corrected myopic Liou and Brennan eye model with different wavelengths

Model	**Wavelength (nm)**		
	486.1	**587.6**	**656.3**
Liou & Brennan	0.150	0.958	0.949

Moving on, compared with the Strehl ratio values on emmetropic model as shown in Table 4, it was found out that the Strehl ratio values of corrected myopic Liou and Brennan were much higher, except for the wavelength of 486.1 nm. The corrective lenses used to correct the refractive error had its refractive index calculated at a wavelength 581.1 nm. Therefore, the Strehl ratio obtained from the wavelength larger than this, i.e., 587.6 nm and 656.3 nm were nearly unaberrated and produced higher values. In contrast, the lower the wavelength (486.1 nm), the Strehl ratio was reduced which exhibited more aberration. It is due to the corrective lenses used to correct the refractive error having its refractive index calculated at a wavelength 581.1 nm. Therefore, the Strehl ratio obtained from the wavelength larger than this, i.e., 587.6 nm and 656.3 nm were nearly unaberrated and produced higher values.

Comparison of Strehl ratios among emmetropic, myopic and corrected myopic of Liou and Brennan (1997) eye model are shown in Table 7. The accuracy between the emmetropia and corrected myopia are also presented. Here, the accuracy is calculated as (corrected value using our myopia model – calculated using emmetropia model)/ corrected value using our myopia model. The accuracy is calculated to verify the improvement of our myopia model compared to the reported model.

Table 7. Comparison of Strehl ratios among emmetropic, myopic and corrected myopic of Liou and Brennan eye model and its accuracy between emmetropic and corrected myopic (B, G and R are blue, green and red wavelengths respectively)

	Emmetropia		**Myopia**	**Corrected Myopia**	**Accuracy**
	Standard Model	**Reported**			
B	0.824	-	0.003	0.150	-4.49
G	0.931	0.820* 0.703**	0.003	0.958	0.03
R	0.846	-	0.004	0.949	0.11

** Bakaraju *et al.* (2008) using visible white light at EPD of 3 mm
* de Almeida & Carvalho (2007) using visible white light at EPD of 2 mm

From Table 7, the Strehl ratio in our study was higher compared with the previous studies (de Almeida & Carvalho, 2007; Zoulinakis *et al.*, 2017). Our study was using blue, green and red wavelengths with EPD of 2.5 mm. Whereas, Bakaraju *et al.* (2008) and de Almeida and Carvalho (2007) were using polychromatic white wavelengths with different EPDs. For the blue wavelength, the Strehl ratio for the corrected myopia was smaller compared to the emmetropic version. This results in an accuracy of -4.49. Whereas the green and red wavelengths for corrected myopia value were higher compared to the emmetropic version. These results showed an accuracy value of 0.03 and 0.11 for the green and red wavelengths, respectively.

In this study, a Strehl ratio was compared for myopia, before and after correction with ophthalmic lenses. A future study can be explored with other types of refractive errors. It is imperative when designing ophthalmic lenses for the correction of other types of refractive errors, namely, hyperopia, astigmatism and presbyopia. A Strehl ratio is one of the factors that can be taken into consideration for achieving a diffraction-limited ophthalmic lens design.

IV. CONCLUSION

From the PSF analysis of this study, the Strehl ratios for all the three wavelengths for the Liou and Brennan model were the highest in the emmetropic model. Whereas, in comparison with emmetropic eye model, the Strehl ratio value of myopic Liou and Brennan was much lower, thus not producing a diffraction-limited system. On further analysis, in comparing with the emmetropic model, it was found out that the Strehl ratio values for all wavelengths of corrected myopic Liou and Brennan were much higher except for the blue wavelength. Hence, the lower the wavelength (486.1 nm), the Strehl ratio was reduced which exhibited more aberration.

In this study, the accuracy of the Strehl ratio for the myopia correction and emmetropia using the Liou and Brennan (1997) model were calculated. It was found that the Strehl ratio accuracy for the blue wavelength was lower. On the other hand, the green and red wavelengths had higher accuracy.

V. ACKNOWLEDGEMENT

This work was partially supported by SEGi Internal Research Fund (Grant no. SEGiIRF/2014-1/FOOPVS-2/15), and the UPM Putra Grants (Grant Nos. GP-IBT/2013/9419200 and GP-IPB/2014/9449902).

VI. REFERENCES

Atchison, DA 2023, Optics of the human eye, 2nd edn, CRC Press. doi.org/10.1201/9781003128601.

Bowrey, HE, Metse, AP, Leotta, AJ, Zeng, G & Mcfadden, SA 2015, 'The relationship between image degradation and myopia in the mammalian eye', Clinical and Experimental Optometry, vol. 98, no. 6, pp. 555-563. doi: 10.1111/cxo.12316.

Bullimore, MA, Gilmartin, B & Royston, J M 1992, 'Steady-state accommodation and ocular biometry in late-onset myopia', Documenta Ophthalmologica, vol. 80, no. 2, pp. 143-155. doi: 10.1007/bf00161240.

Carlson, NB & Kurtz, D 2016, Clinical procedures for ocular examination, 4th edn, McGraw-Hill, New York, USA.

Chua, SY-L, Sabanayagam, C, Tan, C-S, Lim, LS, Toh, J-Y, Chong, Y-S, Gluckman, PD, Yap, F, Cheng, CY, Ngo, CS, Wong, TY, Chong, MFF, Saw, SM & the GUSTO Study Group 2018, 'Diet and risk of myopia in three-year-old Singapore children: the GUSTO cohort', Clinical and Experimental Optometry, vol. 101, no. 5, pp. 692-699. doi: 10.1111/cxo.12677.

De Almeida, MS & Carvalho, LA 2007, "Different schematic eyes and their accuracy to the in vivo eye: A quantitative comparison study', Brazilian Journal of Physics, vol. 37, no. 2a, pp. 378-387. doi: 10.1590/s0103-97332007000300008.

Elliot, DB 2020, Clinical procedures in primary eye care, 5th edn, Elsevier.

Goss, DA & West, RW 2002, Introduction to the optics of the eye, Butterworth-Heinemann, Boston, USA.

Grosvenor, T & Scott, R 1991, 'Comparison of refractive components in youth-onset and early adult-onset myopia', Optometry and Vision Science, vol. 68, no. 3, pp. 204-209. doi: 10.1097/00006324-199103000-00008.

Gwiazda, J, Wendy, L, Marsh-Tootle, Hyman, L, Hussein, M, Norton, TT & the COMET Study Group 2002, 'Baseline refractive and ocular component measures of children enrolled in the correction of myopia evaluation trial (COMET)', Investigative Ophthalmology and Visual Science, vol. 43, no. 2, pp. 314-321.

Hiraoka, T, Kotsuka, J, Kakita, T, Okamoto, F & Oshika, T 2017, 'Relationship between higher-order wavefront aberrations and natural progression of myopia in schoolchildren', Scientific Reports, vol. 7, no. 7876. doi: 10.1038/s41598-017-08177-6.

Jiang, B-C & Woessner, WM 1996, 'Vitreous chamber elongation is responsible for myopia development in a young adult', Optometry and Vision Science, vol. 73, no. 4, pp. 231-234. doi: 10.1097/00006324-199604000-00003.

Liou, H-L & Brennan, NA 1997, 'Anatomically accurate, finite model eye for optical modeling', Journal of the Optical Society of America A, vol. 14, no. 8, pp. 1684-1695. doi: 10.1364/josaa.14.001684

Liu, Y & Wang, Y 2019, 'Optical quality comparison between laser ablated myopic eyes with centration on coaxially sighted corneal light reflex and on entrance pupil center', Journal of the Optical Society of America A, vol. 36, no. 4, pp. B103. doi: 10.1364/josaa.36.00b103.

McBrien, NA & Millodot, M 1987, 'A biometric investigation of late onset myopic eyes', Acta Ophthalmologica, vol. 65, pp. 461-468. doi:10.1111/j.1755-3768.1987.tb07024.x.

Ottevaere, H & Thienpont, H 2005, 'Optical microlenses', eds DG Robert, in *Encyclopedia of modern optics*, Elsevier, pp. 21-43. doi.org/10.1016/B0-12-369395-0/00923-4.

Smith, G, Bedggood, P, Ashman, R, Daaboul, M & Metha, A 2008, 'Exploring ocular aberrations with a schematic human eye model', Optometry and Vision Science, vol. 85, no. 5, pp. 330-340. doi: 10.1097/opx.0b013e31816c4449.

Sun, Y, Xu, F, Zhang, T, Liu, M, Wang, D, Chen, Y & Liu, Q 2015, 'Correction: Orthokeratology to control myopia progression: A meta-analysis', Plos One, vol. 10, no. 6, pp. e0130646. doi: 10.1371/journal.pone.0130646.

Thibos, LN & Bradley, A 1999, 'Modelling the refractive and neuro-sensor systems of the eye', eds P Mouroulis, in Visual instrumentation: Optical design and engineering principles, McGraw-Hill, New York, USA, pp. 101–159.

Zadnik, K & Mutti, DO 2019, 'Outdoor activity protects against childhood myopia - Let the sun shine in', JAMA Pediatrics, vol. 173, no. 5, pp. 415-416. doi: 10.1001/jamapediatrics.2019.0278.

Zapata-Díaz, JF, Radhakrishnan, H, Charman, WN & López-Gil, N 2019, 'Accommodation and age-dependent eye model based on in vivo measurements', Journal of Optometry, vol. 12, no. 1, pp. 3-13. doi: 10.1016/j.optom.2018.01.003.

Zemax User's Manual 2012, Zemax 12 optical design program, Radiant Zemax LLC, Kirkland, USA.

Zoulinakis, G, Esteve-Taboada, JJ, Ferrer-Blasco, T, Madrid-Costa, D & Montés-Micó, R 2017, 'Accommodation in human eye models: A comparison between the optical designs of Navarro, Arizona and Liou-Brennan', International Journal of Ophthalmology, vol. 10, no. 1, pp.43-50. doi:10.18240/ijo.2017.01.07.